A Demonstration of the Optical Rotatory Dispersion of Sucrose

A. Renn (and D. Quirk)
L2 Laboratory Skills and Electronics, Lab Group PH228, Tuesday

Submitted: March 30, 2020, Date of Experiment: February 4, 11, 18, 2020

The specific optical rotation (SOR) of sucrose is measured to be 57.7 $\pm$ 1.3° dm^{-1} g^{-1} cm^3 for 637 nm light at a temperature of 20° C, where the literature value is 56.31° dm^{-1} g^{-1} cm^3, showing reasonable agreement. SOR is also measured for three more wavelengths of light and all are tested against the Drude model for optical rotation, resulting in a good overall fit. Optical rotation is proved to be a versatile technique for calculating the concentration of a sucrose solution. [Sessions 4, 5 & 6 lost to strike action]

1. INTRODUCTION

Optical rotation is a phenomenon in optics which was first observed by Jean-Baptiste Biot in 1815. He discovered that when passing polarised light through an organic substance the axis of polarisation was rotated based on the concentration of the substance [1]. It turned out, as discovered by Louis Pasteur, that the molecules creating such rotation were chiral molecules, which natural sugars happened to be [2]. A necessary starting point for the discussion of optical rotation is Malus' Law, the relation between the intensity of polarised light before (I_0) and after (I) passing through a polarising filter. The relation is such that

$$I = I_0 \cos^2(\theta), \tag{1}$$

where θ is the angle of the polariser with respect to the angle of the polarised light [3]. This results in the fact that a polariser can be rotated 90° to reduce polarised light from maximum intensity to zero intensity, and a further 90° rotation resets the intensity to its initial conditions.

It was also apparent that the optical rotation of light for a certain substance changes depending on the wavelength of that light [4]. This is because optical rotation is dependent on the refractive indices of a material for left and right-handed circularly polarised light, so different wavelengths of light have different refractive indices, which is the case in refractive optics [3]. Finally, optical rotation is also temperature-dependent [5], as the change in vibration of the chiral molecules with temperature gives rise to a change in refractive index, resulting in a change in the rotation of polarised light. Thus, the specific optical rotation of a material is defined as the optical rotation at a specific wavelength of light λ and a specific temperature T as

$$[\alpha]^T_\lambda = \frac{\theta L}{c}, \tag{2}$$

where θ is the optical rotation resulting from a substance of concentration c and with the light passing through a distance L in the material [4]. For example, say the specific optical rotation of D-glucose at 20 °C and 589 nm (the sodium D-line) is α = +52.7° dm^{-1} g^{-1} cm^3. The '+' refers to the fact that the light is rotated anti-clockwise when looking into the beam, while a '-' would mean a clockwise rotation. This would mean that polarised 589 nm light running through 10 cm of a D-glucose solution of concentration 1 g cm^{-3} would be rotated 52.7° anticlockwise, looking into the beam.

This optical rotation was known about for many years, but it was Paul Drude who proposed a model for the optical rotatory dispersion [4]. His model relating optical rotation α to light wavelength λ (still at a specific temperature T) is:

$$[\alpha]^T(\lambda) = \frac{A}{\lambda^2 - \lambda_0^2}, \tag{3}$$

where A and λ_0 are constants. T. Lowry and E. Richards [4] found these constants for sucrose to be A = 2.1648 $\times$ 10^7 ° nm^2 dm^{-1} g^{-1} cm^3 and λ_0 = 146 nm, which will be used in this report as literature values.

2. METHODS

In this experiment, an alterable six-wavelength HEXA-BEAM laser was shone down an optical track through many instruments, as seen in Figure 1. The first of these was a static polarising lens, which ensured that the laser beam was uniformly linearly polarised in the vertical direction. This light then passed through a tube of sucrose solution, of measured length L. In this experiment, first distilled water containing no sucrose was used as a control and reference data. Then, a solution was created of 475.8 g L^{-1} by filling a flask containing 237.9 g of sucrose with distilled water until it measured 500 ml, then mixing thoroughly. This solution was then experimentally tested, from which the next solution was made: a flask of 400 ml of this master solution mixed with 100 ml of distilled water. This resulted in a sucrose solution of concentration 380.6 g L^{-1}. This was repeated to make two more solutions - 304.5 g L^{-1} and 243.6 g L^{-1}. Overall five solutions of different concentrations were created and each tested in the setup with as many wavelengths as time allowed. These were 406 nm (tested with the first three solutions), 520 nm (all five solutions), 637 nm (all five solutions), and 680 nm(first three solutions).

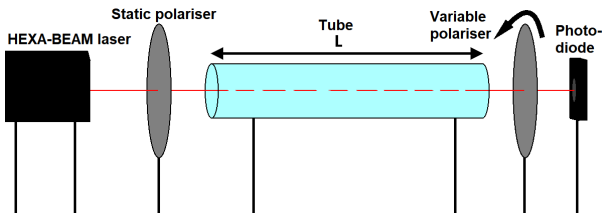

FIG. 1: A diagram of the experimental setup. From left to right: a HEXA-BEAM six-colour 5 mW laser; a static polarising lens; a glass tube of length L, filled with a sucrose solution; a variable polariser; and a photodiode.

After passing through the tube of water and being rotated (or not, in the case of the distilled water), the polarised light then passed through a variable polarising filter controlled by

a computer. This reduced the intensity of the light in accordance with Malus' Law (Equation 1), which was then measured by a photodiode connected to a data-acquisition box connected to the same computer. For each different wavelength and solution concentration, the computer rotated the polariser through 180°, stopping after every 4°, and measured the voltage and error at each angle, for a total of 46 data points per run. 180° was chosen as a range because over 360° the pattern of intensities has two periods as the period of cosine-squared (Malus' Law - Equation 1) is only 180°, which is enough to determine the fitting parameters needed. At each angle, the polariser stopped for 0.25 s in order to capture any voltage fluctuation, and measured 64 samples at a sample rate of 256 s^{-1}. The mean and standard error of these values was taken for each angle (see Errors Appendix) and recorded digitally. This data was saved, and the experiment reset with a different wavelength of light, or concentration of solution, and the process repeated.

With each dataset, χ^2-minimisation was performed to find the best fit for each distribution. The model used for this was

$$V = V_0 + A\cos^2(\theta + \varphi), \tag{4}$$

where V is the voltage measured by the photodiode, V_0 is background voltage, A is the intensity-amplitude, θ is the angle of the polariser, and φ is the phase shift of the rotation. This equation is a more generalised form of Malus' Law (Equation 1). The fitting parameters V_0 and A are used to find the best-fit line. φ was calculated for each different concentration and plotted against concentration to form a linear graph in accordance with Equation 2, where α_λ^T and L are constant in this investigation. The best-fit line of this linear graph was calculated and the gradient and associated error, along with the measured length of the tube, was used to calculate α_λ^T - the specific optical rotation. This analysis was repeated for each of the four wavelengths, resulting in four different values of optical rotation, at four different wavelengths of light.

Finally, throughout the experiment, the temperature of the sucrose solution was monitored as a control. Optical rotation is slightly temperature dependent [5], so an error was introduced into the specific optical rotation based on the temperature difference when it was to be compared against literature values, as these are given at a specific temperature of 20° C.

3. RESULTS

Temperature	Specific Optical Rotation (° dm^{-1} g^{-1} cm^3)
22° C	57.7 ± 1.1
20° C	57.7 ± 1.3
Drude Model	56.31

TABLE I: Values of specific optical rotation and their associated uncertainties obtained with data from the 637 nm light. The methods used to calculate the uncertainties are described in Appendix I.

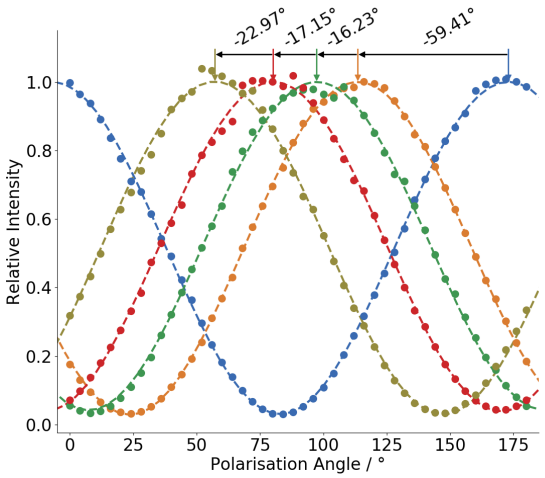

FIG. 2: The effect of sucrose concentration on optical rotation for 637 nm light. From left to right, for the first 5 peaks, concentrations are 0, 475.8, 380.6, 304.5, and 243.6 g L^{-1}. Note error bars are too small to see - a residual plot is provided below.

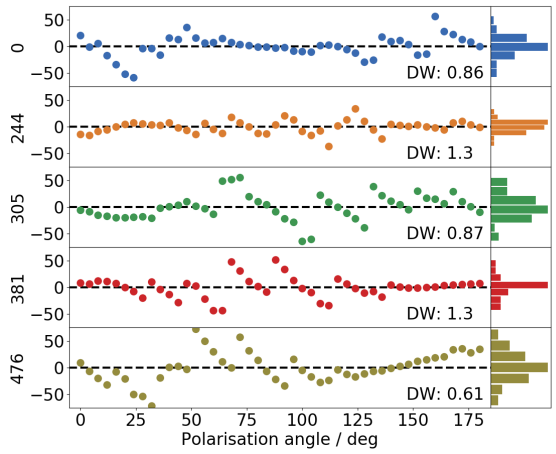

FIG. 3: The normalised residual plot for each curve in Figure 2. Axes labels are the concentrations in g L^{-1}. Note the non-random nature of each curve. A Durbin-Watson statistic is provided for each.

Figure 2 shows the measured photodiode voltages across the range of 180°, with each curve representing a different concentration, for 637 nm light. A χ^2 fit is also shown for each. The rotation from one concentration to the next is annotated. The voltage is normalised to the maximum voltage of the fitted curve over the 180° range. Figures 3 and 4 show the normalised residuals for these curves as a conventional plot, and a lag plot, respectively. Each also displays a Durbin-Watson statistic for all concentrations.

Figure 5 is a polar representation of the data from Figure 2, with an extended range over all polarisation angles with theoretical curves in the region where no data was collected. Once again, the rotation from one concentration to the next is labelled.

The length of the tube of water was measured to be (42.4±0.7) cm. This, along with all data from the 637 nm intensity distributions was used to calculate the specific optical rotation of sucrose at 637 nm and 22 ° C, displayed in

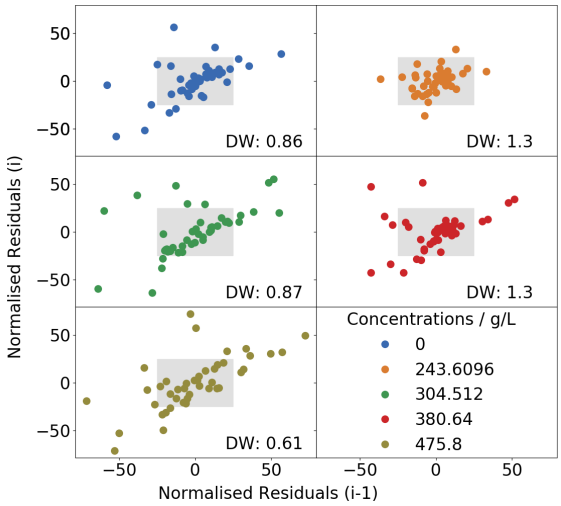

FIG. 4: A lag plot of the residuals from Figure 3. Concentrations are ordered top left rightwards in the order from Figure 3. Bounding box from -25 to 25 shown for comparison between plots. Note the linear pattern of most plots.

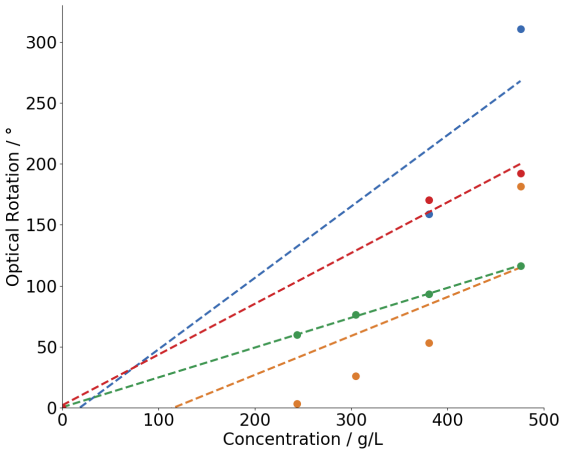

FIG. 6: The change in optical rotation based on concentration for four separate wavelengths. Plotted also is the linear regression line for each. Wavelengths are 520, 637, 680, and 406 nm from the bottom to the top fit line.

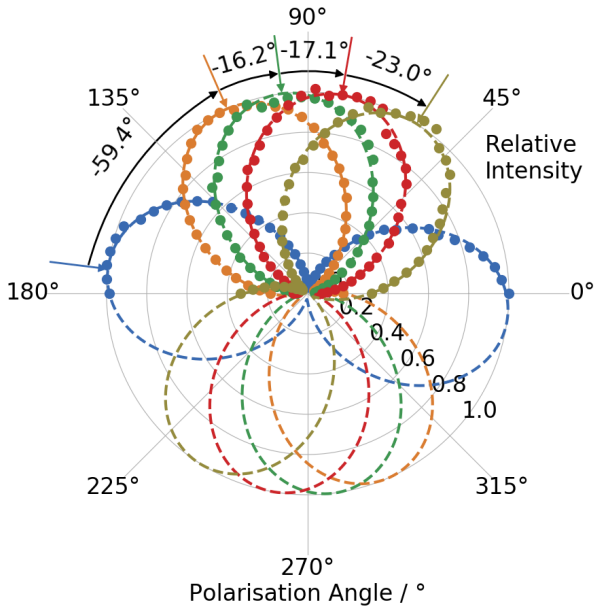

FIG. 5: A polar representation of intensity based on polarisation angle for different sucrose solutions. The first 5 peaks from 180° clockwise are concentrations of 0, 243.6, 304.5, 380.6, and 475.8 g L^{-1}. Figure 5 shows the same data from Figure 2 with the model extended over a 360° range.

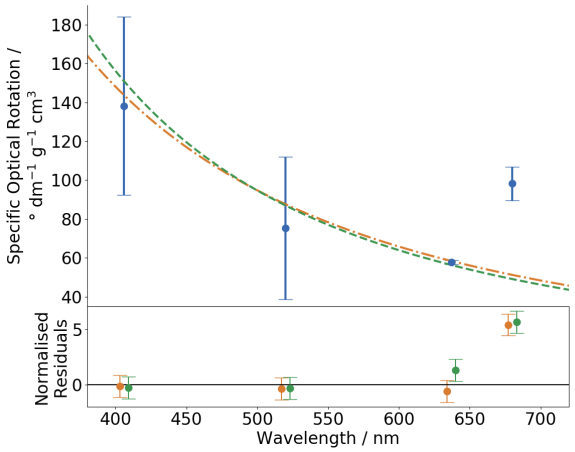

FIG. 7: Measured optical rotatory dispersion. Dashed (green) line is with Drude model parameters [4], dot-dashed (orange) line is a χ^2-fitted line ($\chi^2_{reduced} = 15.1$). Residuals are separated for clarity.

Table I. Also displayed here is the estimated specific optical rotation at 20 ° C as well as a literature value for 637 nm light calculated with the Drude model and accepted coefficients [4].

Figures 6 and 7 expand the discussion towards optical rotatory dispersion. The experiment and χ^2 fitting with the 637 nm experiment was repeated with several other wavelengths. Plotted in Figure 6 is the rotation between the curve of distilled water and of specific concentrations, found from the fitting parameters (for example, with 637 nm light, the 243.6 g L^{-1} solution rotated the light by 59.4°, as seen clearly in Figure 5), for four different wavelengths. The gradients of these lines were found using least squares regression, and along with the value of the length of the rod a value for specific optical rotation was calculated for each (as with in Table I). These values and associated errors are plotted in Figure 7, along with a prediction line from the Drude model parameters and a χ^2 fit line, although this is just for illustrative purposes as there were not deemed enough points for our own values of the Drude constants to be found reliable.

4. DISCUSSION

Figure 2 shows visually that Malus' Law holds true in our experiment, as the rotary intensity distribution follows a cosine-squared fit very well. The minimised χ^2 value is very large, but this can be attributed to the small size of the errors in the voltage, seen more clearly in Figure 3. This is a result of unaccounted-for error as the voltage measurements

made by the photodiode were very accurate and precise, but the voltages did not align perfectly with the fit as seen in the figure. Therefore, unless Malus' Law were to be incorrect there must be unaccounted-for error, such as differently polarised light being incident slightly differently on the photodiode, therefore registering a slightly wrong value, or some nonlinearity in the photodiode.

Another potential source of noise is from the background: when the desk lamp was left on a slow (f $\approx$ 0.2 Hz) signal was seen on the oscilloscope. So, during the experiment, a similar noise could have been present as the door to the corridor which was well-lit was opened throughout the 90 seconds of experimental procedure. Some evidence of a signal similar to this can be seen in Figure 3 as a periodic pattern of residuals, as the axis of polarisation angle is by proxy also an axis of time. This is also visible on Figure 4 as a lag plot; it can be seen that the residuals are not randomly distributed as the lag plots show a linear trendline. The Durbin-Watson statistics of each is also far from two, showing again that the residuals are not normally distributed.

Despite the very small errors, a fit was found along with parameter values and associated errors. These were used to create a model curve, which is best visualised by Figure 5, as this polar plot can literally represent twisting a polariser. One point of consideration is that as concentration is increased, the optical rotation is anti-clockwise. This is just a result of convention, as our polariser was facing towards the laser, where convention has it facing away from the laser, as if you are looking straight into the beam. This just has the result of multiplying all values of optical rotation by -1. A final point to note is that a completely theoretical consideration would have intensity go to zero when the two polarisers are normal to one another, however as seen in Figures 2 and 5 this was not the case. This was because of background light and also a base-voltage level for the photodiode. This was accounted for by including a constant in the fitting function.

Due to time constraints the 637 nm data was the only data collected with a high standard of quality control, but data for several other wavelengths was also taken. There was only enough time, however, for three experiments to be run on some of these secondary wavelengths, so not much data was collected. The same analysis for the first few figures discussed was also applied to these extra wavelengths of 406, 520, and 680 nm, the results of which are shown in Figure 6. Plotted for each wavelength is the difference in the fitted phase parameter of an experiment with a certain concentration and the same experiment with distilled water, resulting in a graph showing the optical rotation based on concentration. Equation 2 was used to justify a straight-line fit for each wavelength. As seen, this line fit works very well for 637 nm, but less well for the other wavelengths. For example, for 520 nm (orange) the first and last points seem to lie on a different line to the middle three points. This may be a result of rushed experimentation, for example a polariser may not have been reset properly or the laser slightly misaligned on subsequent runs. However, this data was deemed apt enough to plot Figure 7.

Figure 7 is an interesting figure as it highlights the phenomenon of optical rotatory dispersion. The first two points have very large errors and the last point is very far from the theoretical model, but the 637 nm data being the most carefully considered data comes with the lowest error and is very close to the Drude model using accepted parameters [4]. A model Drude function was fit with χ^2 minimisation, but there were deemed too few points and not careful previous analysis for meaningful parameters to be extracted from this fit.

Finally, Table I contains the final specific optical rotation calculated using the 637 nm data. This data was used because it was the most scrutinised during laboratory sessions and so the most reliable data to draw conclusions from. Under temperature considerations, the value calculated was kept the same but the error adjusted to account for the 2 °C change. This final value is in good acceptance with the value calculated for 637 nm from literature Drude model coefficients [4]. This shows that the experiment was a success for 637 nm and, with more time, similar analysis could have been done with the different wavelengths and our own personal Drude parameters could have been calculated. If all laser wavelengths had been used, and more concentrations had been tested, this could have been done, as well as reducing overall error on specific optical rotation and Drude parameter calculations.

5. CONCLUSIONS

In conclusion, this report illustrates how effective optical rotation can be as a tool of determining the concentration of a solution of a known substance, or the reverse - the nature of a substance given a known concentration by use of a table of values of specific optical rotation for common substances. This ease, along with the low requirements for conducting the experiment - just a light source, polarising lenses, and a light detector - make optical rotation very applicable to industry, such as testing for sugar-levels in food.

With more time, the technique could have been applied to more complex situations, such as to investigate Faraday's Law [6]. This would require a relatively low-strength magnet (e.g. 0.1 T) and a material with a high Verdet constant (e.g. flint glass, olive oil), both obtainable in an undergraduate laboratory setting.

REFERENCES

[1] J. Applequist (1987). Optical activity: Biot's bequest. (Jean Baptiste Biot; optical rotation in biological substances). American Scientist, 75, 58.

[2] J. Gal (2011). Louis Pasteur, language, and molecular chirality. Chirality, 23(1), 1-16.

[3] C. S. Adams & I. G. Hughes (2019). Optics f2f: From Fourier to Fresnel. Oxford University Press.

[4] T. Lowry, & E. Richards (1924). The rotatory dispersive power of organic compounds. Part XIII. Rotatory dispersion of camphorquinone and of sucrose. Journal of the Chemical Society, Transactions, 125(0), 2511-2524.

[5] H. Wiley (1899). The influence of temperature on the specific rotation of sucrose and method of correcting readings of compensating polariscopes therefor. Journal of the American Chemical Society, 21(7), 568-596.

[6] D. Carr, N. Spong, I. G. Hughes, & C. Adams (2020). Measuring the Faraday effect in olive oil using permanent magnets and Malus' law. European Journal of Physics, Volume 41, Issue 2, p025301

Appendix A: Errors Appendix

1. Measurement Uncertainties

The standard errors on measurements with a ruler were taken to be half an analogue division of the ruler used. When the length of the tube was measured, the errors on each end were combined in quadrature in accordance with the equation,

$$\alpha_L = \sqrt{\alpha_{L_1}^2 + \alpha_{L_2}^2}, \tag{A1}$$

where α_{L_1} and α_{L_2} are the uncertainties on each end of the ruler, and α_L is the final uncertainty on the final length measurement L. [This equation, like all of the equations included in Appendix A, is based on the error analysis formula given in I. G. Hughes and T. P. A. Hase, *Measurements and Their Uncertainties*, Oxford University Press: Oxford (2010).]

The voltage of the photodiode was measured from a data-acquisition box connected to a PC, and multiple measurements were automatically taken at a frequency over a certain time period (described in methods section). These measurements were combined by calculating the mean and standard error of the individual measurements. The mean is calculated using the equation,

$$\bar{V} = \frac{1}{N}\sum_{i=1}^{N} V_i, \tag{A2}$$

where $\bar{V}$ is the mean measurement of the voltage V and V_i are individual measurements of V.

The sample standard deviation, σ_{sample}, of the set of measurements is worked out using the equation,

$$\sigma_{sample} = \sqrt{\frac{1}{N-1}\sum_{i=1}^{N} d_i^2}, \tag{A3}$$

where $d_i = \bar{V} - V_i$. The uncertainty in the measurement of $\bar{V}$ is taken to be its standard error, α_V, where

$$\alpha_V = \frac{\sigma_{sample}}{\sqrt{N}}. \tag{A4}$$

2. χ^2-Minimisation for Parameter Fitting

The χ^2 statistic for a fit of y against x of y(x) is,

$$\chi^2 = \sum_i \frac{(y_i - y(x_i))^2}{\alpha_i^2}, \tag{A5}$$

where $y(x_i)$ is the measurement of y at x_i, y_i is the corresponding value from the fit (linear in this case), and α_i is the standard error on the i$^{\text{th}}$ data point. In this experiment, this statistic is minimised using computer software to determine a best-fit for the data points. An error on this fit is determined by the extremum of the $\chi^2 + 1$ contour on a contour plot of χ^2 with the fit parameters used.

3. Error propagation

In the case of Equation 2, two values, both with intrinsic errors, must be combined to calculate another value with error. In this report, this is achieved via the functional method. Consider two variables A and B with associated errors α_A and α_B respectively. Consider also a third variable Z which is dependent on both A and B such that $Z = f(A, B)$. α_Z, the error in Z, can be calculated numerically with the formula

$$\begin{aligned}(\alpha_Z)^2 = &[f(A + \alpha_A, B) - f(A, B)]^2 \\ &+[f(A, B + \alpha_B) - f(A, B)]^2.\end{aligned} \tag{A6}$$

The values of specific optical rotation in table 1 were calculated precisely in this way.

4. The Durbin-Watson Statistic

The Durbin-Watson statistic can be used to determine whether a set of residuals is randomly distributed. Given a set of residuals R_i, the Durbin-Watson statistic is given by

$$\mathcal{D} = \frac{\sum_{i=2}^{N}[R_i - R_{i-1}]^2}{\sum_{i=1}^{N}[R_i]^2}. \tag{A7}$$

Due to the nature of its creation $\mathcal{D}$ can only take values between 0 and 4. If $\mathcal{D} \approx 2$, then the residuals are randomly distributed and follow a Gaussian distribution. If this is not the case and $\mathcal{D}$ is closer to 0 or 4 then the residuals are systematically correlated or anticorrelated, respectively.